

## Marangoni elasticity of flowing soap films

Ildoo Kim\* and Shreyas Mandre

*School of Engineering, Brown University, Providence, Rhode Island 02912, USA*

(Received 3 October 2016; published 28 August 2017)

We measure the Marangoni elasticity of a flowing soap film to be 22 mN/m irrespective of its width, thickness, flow speed, or the bulk soap concentration. We perform this measurement by generating an oblique shock in the soap film and measuring the shock angle, flow speed, and thickness. We postulate that the elasticity is constant because the film surface is crowded with soap molecules. Our method allows nondestructive measurement of flowing soap film elasticity and the value 22 mN/m is likely applicable to other similarly constructed flowing soap films.

DOI: [10.1103/PhysRevFluids.2.082001](https://doi.org/10.1103/PhysRevFluids.2.082001)

Stationary and flowing soap films are an ideal experimental device to simulate two-dimensional (2D) flows. The development of a soap film channel as a scientific instrument [1–5] expedited the exploration of fundamental fluid dynamics problems using 2D hydrodynamics. Applications include investigations of cylinder wakes [6–9], the flow past flapping flags [10,11], 2D decaying and forced turbulence [12–16], and 2D pipe flow [17].

The persistence of a freely suspended soap film and its mechanical stability is because of soap molecules acting as surfactants [18,19]. The Marangoni effect arising from the surfactant imparts an elasticity<sup>1</sup>  $E = A(d\sigma/dA)$  to the soap film; an increase in the area  $A$  of a patch of the film, which necessarily accompanies film thinning, causes the surfactant molecules to spread apart and the surface tension  $\sigma$  to increase. This increase provides a restoring force that tends to dynamically recover the original area of the film. In this manner, the same mechanism that stabilizes the soap film also imparts a compressible character to the 2D flow in the film. This compressible character is integral to, and therefore an unavoidable consequence of, the mechanism that stabilizes the film. The degree of compressibility is quantified by comparing the characteristic soap film flow speed  $u$  with the Marangoni wave speed  $v_M = \sqrt{2E/\rho h}$ ,<sup>2</sup> where  $\rho$  is the fluid density and  $h$  is its thickness [18,19,22,23,25]. If  $\text{Ma} \equiv u/v_M \ll 1$ , then the inertial forces in the film are too weak to overcome the elastic forces and the film is assumed to approach incompressibility [26].<sup>3</sup>

The objective of this paper is twofold; to present a simple method to measure the Marangoni wave speed and to use the measured values to characterize the film elasticity. Despite the widespread use of soap films for simulating 2D fluid system, neither  $v_M$  nor  $E$  is typically measured or reported. It is desirable to monitor  $v_M$  given that it may change with the operational parameters of the

\*ildoo\_kim@brown.edu

<sup>1</sup>This definition of elasticity is different from the *film* elasticity  $E_f = 2A(d\sigma/dA)$  used in some literature [18,20,21]. The factor 2 in the film elasticity reflects the fact that the film has two surfaces. Then the Marangoni wave speed  $v_M = \sqrt{2E/\rho h} = \sqrt{E_f/\rho h}$  [21]. We follow the convention of the original derivation in Refs. [22,23].

<sup>2</sup>The relation is valid when (i)  $2E \gg \sigma k^2 h^2/2$ , where  $k$  is the wave number of the wave, which justifies the neglect of waves driven by Laplace pressure, and (ii)  $2E \gg 4\eta^2 k^2 h/\rho$ , where  $\eta$  is the viscosity, which justifies the neglect of fluid viscosity. Using  $\sigma \simeq 30$  mN/m,  $k \simeq 2\pi(0.05 \text{ cm})^{-1}$ ,  $h \simeq 10^{-3}$  cm, and  $\eta = 0.1 \text{ cm}^2/\text{s}$  (a conservative overestimate to take into account the film surface viscosity [7,24]), our soap films satisfy both criteria.

<sup>3</sup>The compressibility is proportional to the square of the Mach number like gas flows. The momentum equation for a steady soap film  $\rho u du = d\sigma/h$  and the definition of elasticity  $d\sigma = -E dh/h = -\rho v_M^2 dh/2$  yield  $dh/h = -2\text{Ma}^2(du/u)$ .

ILDOO KIM AND SHREYAS MANDRE

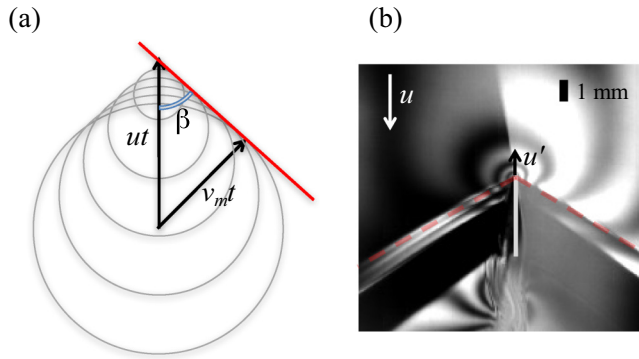


FIG. 1. (a) If a source of the wave is moved by  $ut$  for a time interval  $t$  and the wave is expanded by  $v_M t$  for the same interval, simple trigonometry shows the relation  $\sin \beta = v_M/u$ . (b) Typical oblique shock in a soap film flow, visualized using a low-pressure sodium lamp. To enhance the experimental range, the thin plate is moved at  $u'$  in a flow of speed  $u$ . Shock is formed at a sharply defined angle (the dashed line serves as a guide for the eye).

soap film and that it could be comparable to the typical velocity scale of the simulated 2D flows. Indeed, based on separate measurements of  $v_M$  (246–362 cm/s [27]) and the typical flow speeds (150–250 cm/s [10], 100–400 cm/s [28], or 270–600 cm/s [29]), the soap film flows may not be assumed to be incompressible. However, techniques presented in the literature to measure  $v_M$  [20,27] are too cumbersome to be adopted for repeated real-time monitoring.

We present a simple technique based on an analogy with compressible gas dynamics [21,27,30–33] to measure the Marangoni wave speed. Our technique involves inserting a thin cylinder (a needle) in the soap film, and if required dragging it through, to generate an oblique shock. Then shock angle  $\beta$  is used to determine  $\text{Ma}$  of the incoming flow. Dragging the needle through the film increases the relative speed and allows the shock to form even when the soap film flow is subcritical, which is analogous to *subsonic* flow. We have found that, with some practice, the needle can be dragged with bare hands; therefore, no additional experimental setup is required.

The relationship between  $\beta$  and  $\text{Ma}$  is derived from a simple geometric construction. The shock formed by the envelope of circular wavefronts, which originate at the obstacle, are advected by the freestream  $u$ , and expand at speed  $v_M$  [see Fig. 1(a)]; this simple construction leads to the relation

$$\sin \beta = \frac{1}{\text{Ma}} = \frac{v_M}{u}. \quad (1)$$

Thus,  $\text{Ma}$  may be estimated by measuring the oblique shock angle  $\beta$ , and an independent measurement of  $u$  yields  $v_M$ . Equation (1) is the special case of a more general  $\alpha - \beta - \text{Ma}$  relation for oblique shocks formed around wedges of angle  $\alpha$  [34]. The soap film flow is shown to be analogous to gas flow with the heat capacity ratio  $\gamma = 1$ . According to this analogy, the surface tension acts analogously to gas pressure, the film thickness is analogous to gas density, and the ratio  $\text{Ma}$  plays a role identical to that of the Mach number in compressible gas dynamics. The corresponding oblique shock relation due to a wedge was presented in a previous study [31].

We also present the Marangoni wave speed measured for soap films created using the commonly used solutions of commercial detergent. We find that the Marangoni wave speed is between 330 and 200 cm/s as the film thickness varies from 4 to 11  $\mu\text{m}$ .

Our measurement of  $v_M$  allows us to conveniently probe the elasticity of soap films; we find that in our setup the soap film elasticity remains constant at  $E = 22$  mN/m. We propose that the constant value of the elasticity is due to the overcrowding of soap molecules on the film surface.

Our soap film channel setup is similar to those previously used by various groups [4,13,28,35]. The channel is vertical, approximately 1.8 m long, and 3 to 6 cm wide depending on experimental

## MARANGONI ELASTICITY OF FLOWING SOAP FILMS

conditions. We use 2% solution of commercial dish soap (Dawn, P&G) in distilled water to form soap films, which is a common recipe. The soap solution flux  $F$  is controlled by adjusting the valve opening at the top of the channel. The valve opening is calibrated to  $F$  by directly collecting the solution per unit time and weighing it, which gives the measurement of  $F$  with up to 5% uncertainty. We work in a section of the soap film where the thickness does not vary with downstream distance, far from any “hydraulic jump” that can form near the end of the channel [28]. The flow speed  $u$  of the channel is determined by particle tracking using high-speed imaging (Photron SA4). Our measurements of  $u$  are compared to separate particle image velocimetry (PIV), and the two measurements agree within 1%. Once  $F$ , the width  $W$ , and  $u$  are determined, we can calculate the thickness of the film using  $h = q/u$ , where  $q \equiv F/W$  is the flux per unit width. We take all of our measurements at the center of the channel, although our method in principle can be used at any part of the soap film channel, provided that  $h$  is considered as local thickness where we measure  $u$ . Our separate measurements of  $h(y)$  using low-pressure sodium lamp interferogram and  $u(y)$  using PIV, where  $y$  is the spanwise coordinate of the channel, reveal that  $q = h(y)u(y)$  is independent of  $y$ . This is also indicated by other studies [28,36].

In the usual experimental conditions,  $q$  is varied from 0.1 to 0.4 cm<sup>2</sup>/s. Under such conditions,  $u$  varies from 250 to 330 cm/s and  $h$  varies from 4 to 11  $\mu$ m. A simple dimensional analysis to balance the gravitational force and air friction implies that  $u \sim q^{2/5}$  and  $h \sim q^{3/5}$  [36], and this is roughly consistent with our observations.

To simulate a wedge of  $\alpha = 0$ , we place a thin plate in the middle of the soap film. The thin plate is 0.4 cm long in the longitudinal direction and 25  $\mu$ m wide in thickness. If the flow speed is greater than the Marangoni wave speed, namely,  $u > v_M$ , an oblique shock is formed on both sides of the  $\alpha = 0$  wedge. Otherwise, when  $u < v_M$ , no shock is observed; we then move the thin plate against the soap film flow along a translational stage at the speed  $u'$  in the laboratory frame. A simple Galilean transformation gives the relative speed  $v$  between the flow and the wedge as  $v = u + u'$ . This technique grants us two important features: to observe oblique shocks when the flow is naturally subcritical and to achieve a greater range of Ma.

We note that our results are reproducible when the  $\alpha = 0$  wedge is replaced by a thin needle. Unlike a thin plate shock, a thin needle shock is insensitive to the angle of attack. Therefore, our scheme can be adopted at no cost and with some practice even without a translational stage.

Figure 1(b) shows a typical oblique shock formed in a soap film channel. The soap film is illuminated by a low-pressure sodium lamp, which has a single wavelength at 589 nm. The use of the monochromatic light source allows us to visualize the shock structure through an interferogram that is very sensitive to the thickness variation. We report that the shock structure is less visible under polychromatic light sources, suggesting that the shock is peristaltic (i.e., varicose) wave.<sup>4</sup>

The peristaltic nature of the shocks is further confirmed by an independent PIV in Fig. 2. In Fig. 2(a), a raw PIV image is shown, where white dots in the black background are passive particles seeded for PIV measurement. Near the tip of the obstacle (bright long object in the right), a shock is faintly visible at  $\beta = 36^\circ$ . We carry out PIV analysis for the region bounded by the red box, away from the static feature in raw images. In Fig. 2(b), the change in velocity from its mean is displayed as a color map. In the map, a straight and thin band of relatively lower velocity is clearly distinguishable and it extends to the tip; therefore, it is evident that it represents the shock. The change in the velocity can be emphasized by calculating the divergence of the field in Fig. 2(c). The blue (red) color represents the negative (positive) divergence, meaning that the soap film is thickening (thinning). Away from the shock, the divergence is measured close to zero.

The PIV measurement clearly shows that the film undergoes thickening and then thinning. When a flow encounters an obstructing object at the speed faster than the wave speed, a sudden change of the flow direction causes the formation of an oblique shock and consequently the film gets thicker.

<sup>4</sup>In this mode, two surfaces of the film are mirrored about the center plane. If the front surface is convex, then the opposing surface viewed from the rear is also convex.

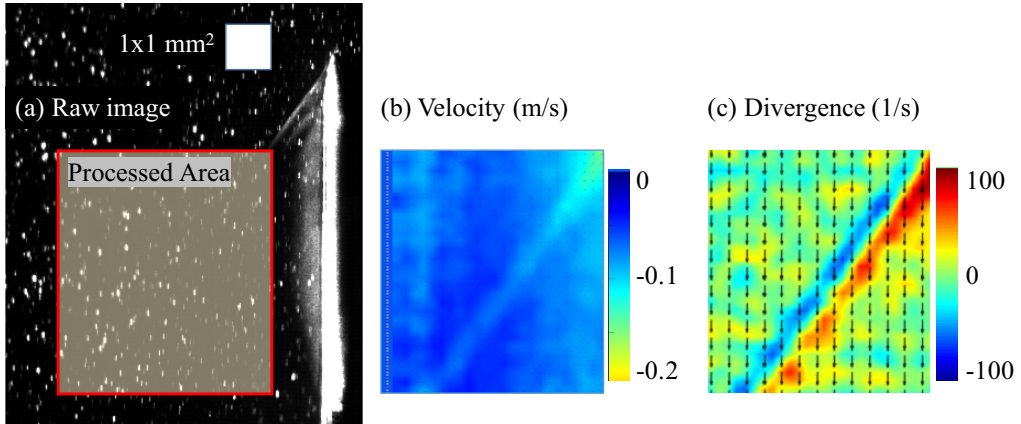


FIG. 2. (a) In the background, a raw PIV image shows that a shock wave formed at  $\beta = 36^\circ$  near the thin plate. (b) When the shock is extrapolated, it coincides with a thin band of region where the velocity is slower than average. (c) Divergence of the velocity field shows that the flow decelerates and accelerates when it bypasses the shock. This result indicates that the film thickness changes across the shock.

As the flow advances further downstream, it accelerates and thins according to a Prandtl-Meyer expansion fan [34]. In our system, the flow direction far from the tip is the same as the incoming flow.

In Figs. 1(b) and 2, we can also see that the shock is very sharply defined; the thickness of the shock is only a fraction of a millimeter, implying that the shock formation time is less than 0.2 ms. Considering that the diffusion coefficient  $D \simeq 4 \times 10^{-6} \text{ cm}^2/\text{s}$  [18], the time scale for soap molecules to diffuse across the thickness varies from 6.7 to 50 ms depending on  $h$ . Based on these estimates, we conclude that the exchange of surfactants between bulk and surface is negligible and that the shock is in the *Marangoni* regime.

As the shock angle  $\beta$  is clearly visible in the interferogram in Fig. 1(b), analyses of such images give the measurements of  $\beta$  as a function of flow conditions. The measurements are repeated six times per flow condition to reduce the uncertainty, which is approximately  $1^\circ$ .

In the prescribed setup, Eq. (1) implies a linear relation between  $1/\sin\beta$  and the relative speed  $v$ , and we find that the linearity is observed only when we group data by their corresponding film thickness. For example, data with  $h = 5.6 \pm 0.1 \mu\text{m}$  are grouped together and displayed in Fig. 3 as circles. As the corresponding solid line indicates,  $1/\sin\beta$  and  $v$  are linearly proportional to each other. By grouping similar cases for other film thicknesses, we find that  $v_M$  is faster in thin films than in thick films. Figure 3 also shows experimental data for  $h = 7.0, 8.0, \text{ and } 9.8 \mu\text{m}$ . Here we find that for all cases the intercept is zero as expected, but the slope varies by the thickness. The slope, which is  $v_M^{-1}$  in our model, is the most gradual for the thinnest film (see circles in Fig. 3) and the steepest for the thickest film (down-pointing triangles).

Figure 4 shows our measurement of the Marangoni wave speed using  $v_M = v \sin\beta$  as a function of  $h$ . In our experiments,  $F$ ,  $W$ , and  $v$  are independently varied, however the measured  $v_M$  depends only on  $h$ . All data points, each collected using different soap solution flux in the range  $0.38 \leq F \leq 1.17 \text{ cm}^3/\text{s}$  and channel width in the range  $3 \leq W \leq 6 \text{ cm}$ , collapse into a single scaling relation  $v_M \propto h^{-1/2}$  in the range for  $h$  spanning a little less than a decade. This clear trend that  $v_M$  is a function of  $h$  but not of  $F$  and  $W$  allows us to calculate the soap film's elasticity using  $v_M = \sqrt{2E/\rho h}$  [18,19,25]. The proportionality constant implies that the elasticity of our soap film is  $E = 22 \pm 1 \text{ mN/m}$ , being independent of  $h$ ,  $F$ , and  $W$ , within our measurement error.

The Marangoni elastic wave is not the only wave that can propagate through a soap film; the bending wave derived by Taylor [25] describes motion in which two interfaces of a film move

## MARANGONI ELASTICITY OF FLOWING SOAP FILMS

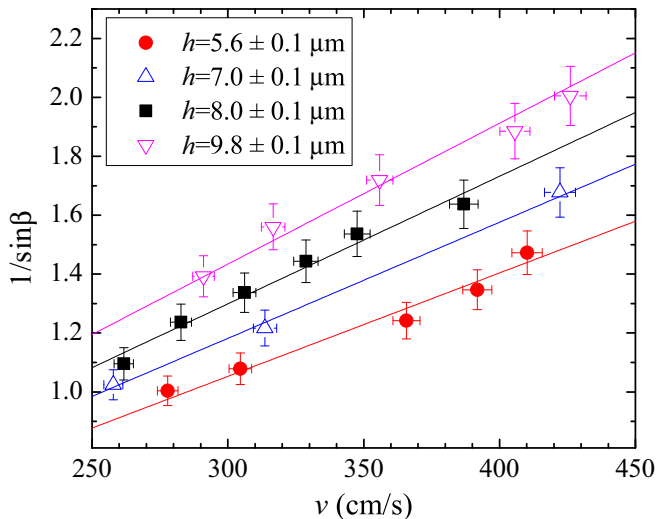


FIG. 3. Plot of  $1/\sin \beta$  vs  $v$  at different film thicknesses. Equation (1) suggests that these two quantities are linearly proportional to each other when the Marangoni wave speed  $v_M$  is constant. Such linearity is observed when experimental data points are grouped by the film thickness  $h$ . For a fixed  $h$ ,  $1/\sin \beta$  is directly proportional to  $v$  with zero intercept and the slope decreases as  $h$  decreases. This relationship implies that the Marangoni wave speed increases as the film gets thinner.

together and propagates at a speed  $v_b = \sqrt{2\sigma/\rho h}$  [18,19,25]. As the surface tension has the same dimensions as elasticity, the bending wave speed has the same functional dependence on the film thickness as the Marangoni wave speed. Using previous measurements [35] of  $\sigma \simeq 32.7$  mN/m, we plotted the resulting  $v_b$  in Fig. 4. The distinction of the bending wave speed from the Marangoni

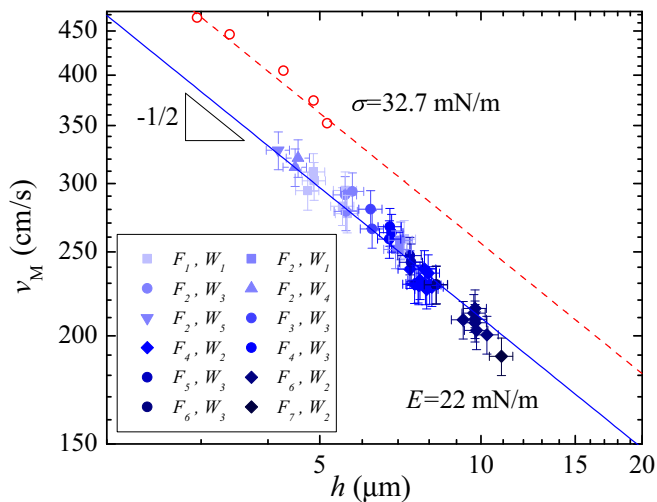


FIG. 4. Marangoni wave speed  $v_M$  vs the film thickness  $h$  (closed symbols). The solid blue line shows  $v_M \sim h^{-0.5}$  corresponding to  $E = 22$  mN/m. The symbol and color stand for different flux and width settings: flux  $F_1 = 0.38$  cm<sup>3</sup>/s,  $F_2 = 0.56$  cm<sup>3</sup>/s,  $F_3 = 0.65$  cm<sup>3</sup>/s,  $F_4 = 0.75$  cm<sup>3</sup>/s,  $F_5 = 0.85$  cm<sup>3</sup>/s,  $F_6 = 0.95$  cm<sup>3</sup>/s, and  $F_7 = 1.17$  cm<sup>3</sup>/s and width  $W_1 = 3$  cm,  $W_2 = 3.5$  cm,  $W_3 = 4$  cm,  $W_4 = 5$  cm, and  $W_5 = 6$  cm. Open circles show measurements of the bending wave speed [35] and the dashed line corresponds to  $\sigma = 32.7$  mN/m.

wave speed determined from the shock wave combined with the PIV observations confirms that we excite the Marangoni shock waves.

Our experimental results furnish us with insight into physics of flowing soap films. The soap film possesses Gibbs elasticity if sufficient time is available for perturbations in soap film concentrations to equilibrate and possesses Marangoni elasticity in the opposite case. The Gibbs elasticity  $E_G = 2RTc/(1 + c_b h/2c)$  [18,19,22,25,37] depends on  $h$  and the bulk concentration  $c_b$  of surfactant in equilibrium with the surface concentration  $c$ . The Marangoni elasticity  $E_M = 2RTc$  depends on  $c$  but not on  $h$  or  $c_b$ . We find that in the range of parameters we are able to establish the soap film, its elasticity does not depend on the soap film width or its thickness. The independence of the measured elasticity on film thickness, the disparate diffusive and shock-formation time scales, our PIV measurements, and the wave speed measurements altogether imply that the shocks we observe are due to Marangoni elasticity.

Furthermore, we experiment with bulk soap concentrations of 1% and 4% in the overhead reservoir and with different size of the nozzle that feeds the soap solution to the film in an attempt to influence the soap film elasticity. We find no noticeable difference in our observation; such modifications vary the elasticity less than 4%, falling within the margin of error.

The constant value for the Marangoni elasticity we measure and its independence on the operational parameters of the flowing soap film implies one of two possibilities: the interface is crowded with soap molecules or  $\sigma \sim \sigma_0 - E(\ln c)/2$  in the parameter regime we examine. The surface tension  $\sigma(c)$  is a function of surface soap concentration, and the accompanying Marangoni elasticity is derived using  $dc/c = -dA/A$  to be  $E = -2cd\sigma/dc$ . The first possibility is that in the parameter regime we explored, the soap molecules crowd the interface, leading to a limiting value  $c = c_\infty$ . The soap concentration in any part of soap film is above the critical micelle concentration, and the surface concentration of soap molecules rapidly approaches the limiting value  $c_\infty$ . Consequently, the elasticity approaches the value of  $-2cd\sigma/dc$  at  $c = c_\infty$ . The alternative is that the form of  $\sigma(c)$  is such that the elasticity  $E$  is a constant, implying  $\sigma \sim \sigma_0 - E(\ln c)/2$ . While we cannot strictly rule out the latter possibility, the former is more likely because it is the simplest explanation consistent with the observations.

We postulate that our observation of the constant elasticity can be generalized, given that most soap film channel setups reported in the literature used the same soap, the same concentration, similar flow rates, and comparable dimensions for the soap film. For such published articles that use the same soap and also report the film thickness, we estimate the Marangoni wave speed by assuming that the elasticity is 22 mN/m. The range of Mach number is then calculated using the range of flow speed cited in each article [9,10,17,28,38–41]. Figure 5 shows the estimated range

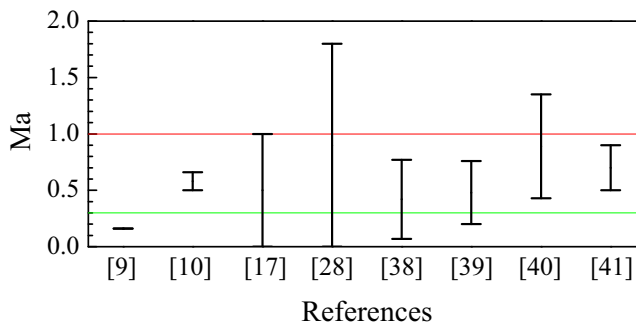


FIG. 5. Elastic Mach numbers are calculated for recent studies [9,10,17,28,38–41] using the same soap as ours. Using the film thickness and  $E = 22$  mN/m, the Marangoni wave speed is calculated and used to normalized the flow speed as specified in the given references. The bar graph shows the lower and upper limits of the Mach number in each study. Horizontal lines indicate  $Ma = 0.3$  and  $1.0$  to guide readers.

MARANGONI ELASTICITY OF FLOWING SOAP FILMS

of  $Ma$  for these studies, which indicates that for the vast majority of the cases the flow is clearly of a compressible nature. One study [28] recognized the compressible nature of the flow and used the Marangoni shock to estimate the compressibility, while the others do not attempt to measure the compressible character of the flow. Our method presents a nonintrusive and low cost method for estimating the Marangoni Mach number *in situ* for a complete characterization of flowing soap films in future investigations. Furthermore, the value  $E = 22 \text{ mN/m}$  may be used to determine the Marangoni Mach number without any experimentation.

To summarize, we provided an experimental method for *in situ* measurement of the Marangoni wave speed. In our method, we artificially generated oblique shocks in soap film flows by introducing an obstruction and determined the Marangoni Mach number by measuring the shock angle. We used the method to make a complete characterization of the soap film's Marangoni elasticity. Our measurements show that the Marangoni wave speed depends on the film thickness and the elasticity is constant for films in our range of experiments independent of film thickness, width, flow rate, or the bulk concentration of surfactants. We suspect that the elasticity is constant in our soap films because the soap concentration is higher than the critical micelle concentration. Considering that it is hard to establish a soap film using a dilute soap solution, we suspect that the reported value of  $22 \text{ mN/m}$  of the elasticity must be universal for all soap films using the same detergent.

APPENDIX: ALTERNATIVE DERIVATION USING THE GAS-DYNAMIC ANALOGY

Here we present a brief derivation of the Marangoni wave speed in soap films. For a more complete derivation, see Refs. [21,22,31,32]. The momentum conservation equation of a soap film flow is

$$\frac{D\vec{u}}{Dt} = \frac{2\vec{\nabla}\sigma}{\rho h}, \tag{A1}$$

where  $h$  is the thickness and  $\vec{\nabla}\sigma$  is the Marangoni stress

$$2\vec{\nabla}\sigma = \frac{2d\sigma}{dh}\vec{\nabla}h = -\frac{2E}{h}\vec{\nabla}h. \tag{A2}$$

Substitution yields

$$\frac{D\vec{u}}{Dt} = -\frac{2E}{\rho h}\frac{\vec{\nabla}h}{h}. \tag{A3}$$

An analogy can be observed with the momentum equation for a compressible gas flow,

$$\frac{D\vec{u}}{Dt} = -a^2\frac{\vec{\nabla}\rho_g}{\rho_g}, \tag{A4}$$

where  $\rho_g$  is the gas density and  $a$  is the speed of sound, with the correspondence  $h \leftrightarrow \rho_g$ . Based on this analogy, the Marangoni wave speed is  $a \leftrightarrow \sqrt{2E/\rho h}$ .

- 
- [1] M. Gharib and P. Derango, A liquid film (soap film) tunnel to study two-dimensional laminar and turbulent shear flows, *Physica D* **37**, 406 (1989).
  - [2] J. M. Chomaz and B. Cathalau, Soap films as two-dimensional classical fluids, *Phys. Rev. A* **41**, 2243 (1990).
  - [3] M. Beizaie and M. Gharib, Fundamentals of a liquid (soap) film tunnel, *Exp. Fluids* **23**, 130 (1997).
  - [4] M. A. Rutgers, X. L. Wu, and W. B. Daniel, Conducting fluid dynamics experiments with vertically falling soap films, *Rev. Sci. Instrum.* **72**, 3025 (2001).

- [5] D. Georgiev and P. Vorobieff, The slowest soap-film tunnel in the Southwest, *Rev. Sci. Instrum.* **73**, 1177 (2002).
- [6] P. Vorobieff and R. E. Ecke, Fluid instabilities and wakes in a soap-film tunnel, *Am. J. Phys.* **67**, 394 (1999).
- [7] P. Vorobieff and R. E. Ecke, Cylinder wakes in flowing soap films, *Phys. Rev. E* **60**, 2953 (1999).
- [8] P. Roushan and X. L. Wu, Structure-Based Interpretation of the Strouhal-Reynolds Number Relationship, *Phys. Rev. Lett.* **94**, 054504 (2005).
- [9] I. Kim and X. L. Wu, Unified Strouhal-Reynolds number relationship for laminar vortex streets generated by different-shaped obstacles, *Phys. Rev. E* **92**, 043011 (2015).
- [10] S. Jung, K. Mareck, M. J. Shelley, and J. Zhang, Dynamics of a Deformable Body in a Fast Flowing Soap Film, *Phys. Rev. Lett.* **97**, 134502 (2006).
- [11] L. Ristroph and J. Zhang, Anomalous Hydrodynamic Drafting of Interacting Flapping Flags, *Phys. Rev. Lett.* **101**, 194502 (2008).
- [12] H. Kellay, X-l. Wu, and W. I. Goldburg, Experiments with Turbulent Soap Films, *Phys. Rev. Lett.* **74**, 3975 (1995).
- [13] B. K. Martin, X. L. Wu, W. I. Goldburg, and M. A. Rutgers, Spectra of Decaying Turbulence in a Soap Film, *Phys. Rev. Lett.* **80**, 3964 (1998).
- [14] M. Rivera, P. Vorobieff, and R. E. Ecke, Turbulence in Flowing Soap Films: Velocity, Vorticity, and Thickness Fields, *Phys. Rev. Lett.* **81**, 1417 (1998).
- [15] M. A. Rutgers, Forced 2D Turbulence: Experimental Evidence of Simultaneous Inverse Energy and Forward Enstrophy Cascades, *Phys. Rev. Lett.* **81**, 2244 (1998).
- [16] Y. Jun and X. L. Wu, Large-scale intermittency in two-dimensional driven turbulence, *Phys. Rev. E* **72**, 035302 (2005).
- [17] T. Tran, P. Chakraborty, N. Guttenberg, A. Prescott, H. Kellay, W. I. Goldburg, N. Goldenfeld, and G. Gioia, Macroscopic effects of the spectral structure in turbulent flows, *Nat. Phys.* **6**, 438 (2010).
- [18] Y. Couder, J. M. Chomaz, and M. Rabaud, On the hydrodynamics of soap films, *Physica D* **37**, 384 (1989).
- [19] J. M. Chomaz, The dynamics of a viscous soap film with soluble surfactant, *J. Fluid Mech.* **442**, 387 (2001).
- [20] A. Prins, C. Arcuri, and M. Van den Tempel, Elasticity of thin liquid films, *J. Colloid Interface Sci.* **24**, 84 (1967).
- [21] C. Y. Wen and J. Y. Lai, Analogy between soap film and gas dynamics. 1. Equations and shock jump conditions, *Exp. Fluids* **34**, 107 (2003).
- [22] J. Lucassen, M. Van den Tempel, A. Vrij, and F. Hasselink, Waves in thin liquid films I. The different modes of vibrations, *Proc. K. Ned. Akad. Wet. B* **73**, 109 (1970).
- [23] A. Vrij, F. Hasselink, J. Lucassen, and M. Van den Tempel, Waves in thin liquid films II. Symmetrical modes in very thin films and film ruptures, *Proc. K. Ned. Akad. Wet. B* **73**, 124 (1970).
- [24] V. Prasad and E. R. Weeks, Two-Dimensional to Three-Dimensional Transition in Soap Films Demonstrated by Microrheology, *Phys. Rev. Lett.* **102**, 178302 (2009).
- [25] G. I. Taylor, The dynamics of thin sheets of fluid. II. waves on fluid sheets, *Proc. R. Soc. London Ser. A* **253**, 296 (1959).
- [26] M. I. Auliel, F. Castro, R. Sosa, and G. Artana, Gravity-driven soap film dynamics in subcritical regimes, *Phys. Rev. E* **92**, 043009 (2015).
- [27] C. Y. Wen, S. K. Chang-Jian, and M. C. Chuang, Analogy between soap film and gas dynamics. 2. Experiments on one-dimensional motion of shock waves in soap films, *Exp. Fluids* **34**, 173 (2003).
- [28] T. Tran, P. Chakraborty, G. Gioia, S. F. M. Steers, and W. I. Goldburg, Marangoni Shocks in Unobstructed Soap-Film Flows, *Phys. Rev. Lett.* **103**, 104501 (2009).
- [29] M. Fayed, R. Portaro, A.-L. Gunter, H. A. Abderrahmane, and H. D. Ng, Visualization of flow patterns past various objects in two-dimensional flow using soap film, *Phys. Fluids* **23**, 091104 (2011).
- [30] C. Y. Wen, Y. M. Chen, and S. K. Chang-Jian, A soap film shock tube to study two-dimensional compressible flows, *Exp. Fluids* **31**, 19 (2001).
- [31] C.-Y. Wen and J.-Y. Lai, Gasdynamics-like equations for oblique shock waves and nozzle flows in soap films, *J. Mech.* **20**, 69 (2004).

## MARANGONI ELASTICITY OF FLOWING SOAP FILMS

- [32] P. Fast, A viscous compressible model of soap film flow and its equivalence with the Navier-Stokes equations, [arXiv:physics/0511175v1](#).
- [33] C. Y. Wen, W. J. Wu, and H. Chen, Shock-vortex interactions in a soap film, *Shock Waves* **18**, 185 (2008).
- [34] H. W. Liepmann and A. Roshko, *Elements of Gasdynamics* (Wiley, New York, 1957).
- [35] I. Kim and X. L. Wu, Tunneling of micron-sized droplets through soap films, *Phys. Rev. E* **82**, 026313 (2010).
- [36] M. A. Rutgers, X. L. Wu, R. Bhagavatula, A. A. Petersen, and W. I. Goldburg, Two-dimensional velocity profiles and laminar boundary layers in flowing soap films, *Phys. Fluids* **8**, 2847 (1996).
- [37] A. I. Rusanov and V. V. Krotov, Gibbs elasticity of liquid films, *Prog. Surf. Memb. Sci.* **13**, 415 (1979).
- [38] S. Alben, M. Shelley, and J. Zhang, Drag reduction through self-similar bending of a flexible body, *Nature (London)* **420**, 479 (2002).
- [39] M. M. Bandi, A. Concha, R. Wood, and L. Mahadevan, A pendulum in a flowing soap film, *Phys. Fluids* **25**, 041702 (2013).
- [40] R. T. Cerbus and W. I. Goldburg, Intermittency in 2D soap film turbulence, *Phys. Fluids* **25**, 105111 (2013).
- [41] J. Zhang, S. Childress, A. Libchaber, and M. Shelley, Flexible filaments in a flowing soap film as a model for one-dimensional flags in a two-dimensional wind, *Nature (London)* **408**, 835 (2000).